Supplementary information

Rotating square tessellations enabled stretchable and adaptive curved display

Yang Deng[1#], Kuaile Xu[2#], Rui Jiao[1], Weixuan Liu[2], Yik Kin Cheung[1], Yongkai Li[1], Xiaoyi Wang[1], Yue Hou[1], Wei Hong[2], Hongyu Yu[1]**

Area utilization analysis

In fact, area utilization is positively correlated with the ratio of **w** and **h**, while negatively correlated with the number of arrays of rotating squares. Here, for the sake of analyzing the relationship between these parameters, we assume that $Nx = Ny =$ n, and that **w** and **h** take three different sets of values as references.

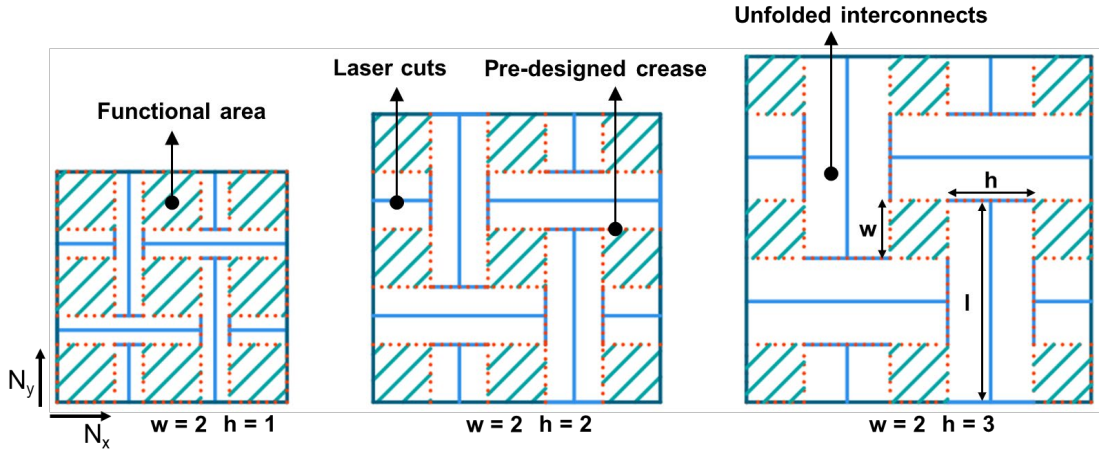

Supplementary Figure 1. The components of the rotating squares structure. Three groups of geometric parameters correspond to different area utilization.

As shown in the Supplementary Figure 1, the components of the rotating squares structure includes functional area (for housing LED ships), laser cuts (for constructing interconnects), pre-designed crease (forming stiffness gradient with the rest of area) and unfolded interconnects. When **n** is equal to 3, area utilization decreases significantly with the increase of width of interconnects. We have calculated the relationship between **n** and **w**, **h**, as shown in the Supplementary Figure 2. When **n** is less than 10, the area utilization decreases sharply with the increase of it, but soon tends to be stable and infinitely approaches the theoretical value. Consequently, as **n** approaches infinity, area utilization is determined by the dimension of **w** and **h**. The commercial numerical analysis software Matlab was used to construct the relation of dimension of **w** and **h** and area utilization when **n** tends to infinity. It can be seen that when the ratio of **w** and **h** reaches about 10, the area utilization rate can reach more than 80% (Supplementary Figure 3). In contrast, area utilization is minimal when the ratio of **w** and **h** is small,

and many manufacturers have taken advantage of this feature to produce stunning transparent screens.

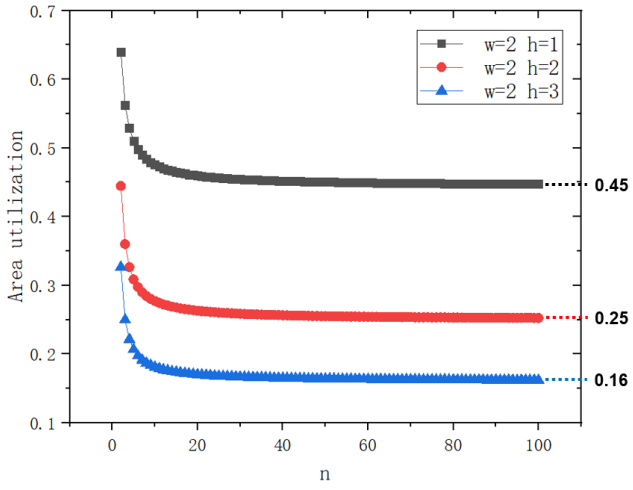

Supplementary Figure 2. The relation between area utilization rate and the 3 series of w and h.

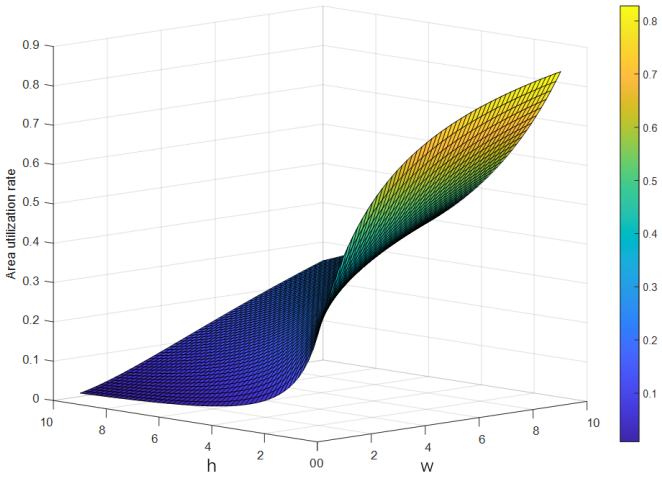

Supplementary Figure 3. Relation of area utilization rate and dimension of **w** and **h,** when **n** tends to infinity, w, h $\in [1, 10]$.

In fact, this strategy of increasing transmittance of device by reducing area utilization has been successfully used by manufacturers to produce transparent screens. Typically, LG Display has proposed a way to change the pixels' microstructure to achieve transparent OLED displays. The screen is divided into opaque areas, which display images, and transparent areas, which allow light to pass through and greatly increase the screen's transparency (about 38%, Supplementary Figure 4b).

Similarly, when the interconnects are vertical, they free up space to allow light to pass through. Here, UV-VIS spectrophotometer (Perkin Elmer, Supplementary Figure 4a)

was used to measure the absorption rate of visible light at 300-800nm in different regions of the display following the equation:

$$A = log_{10}\left(\frac{I_0}{I}\right) = 2 - log_{10}(\%T) \qquad (1)$$

Where I is transmitted light ("output") and I_0 is incident light ("input"), transmittance (T) is the fraction of incident light which is transmitted.

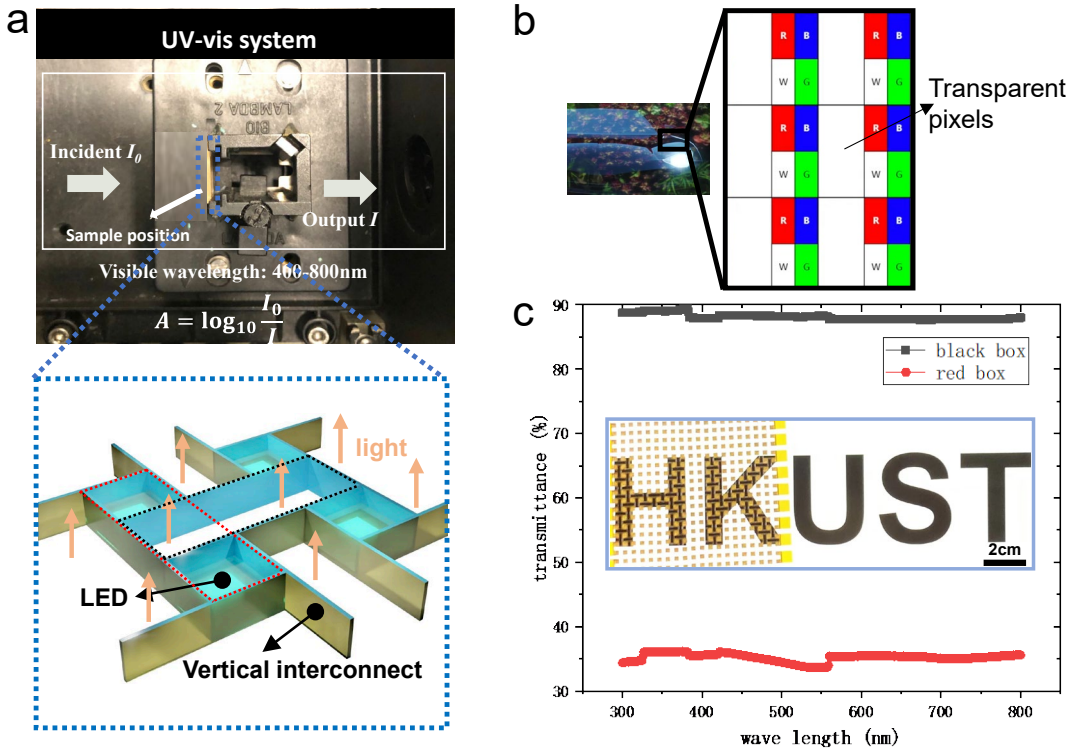

Supplementary Figure 4. **a** Optical image of original display on UV-VIS spectrophotometer. The inset shows a schematic of light passing through the hollow region. **b** Transparent OLED display. **c** The light transmittance of the red box area and the black box area. The inset shows an optical picture of letters still visible when blocked by the device.

As shown in the Supplementary Figure 4a, we tested the light absorption rate of the functional area (marked with red box) and hollow area (marked with black box) of the display. According to the formula, we get the transmittance of these two areas is 35% and 89% respectively (Supplementary Figure 4c). Combined with the area utilization rate, we estimate that the overall transmittance of the display is about 67%. With excellent light transmittance, the image blocked by the device can be clearly seen without backlight (the inset of Supplementary Figure 4c).

Stretchability analysis

Because the rotating squares structure connected by vertical interconnects can be stretched or compressed, its stretchability analysis is much more complicated than that of rigid joints. Similarly, the stretchability of the structure determined by three parameters: **n**, **w**, and **h**. Taking 3 × 3 squares as an example, it is apparent that the larger the spacing **h** is, the greater its stretchability will be.

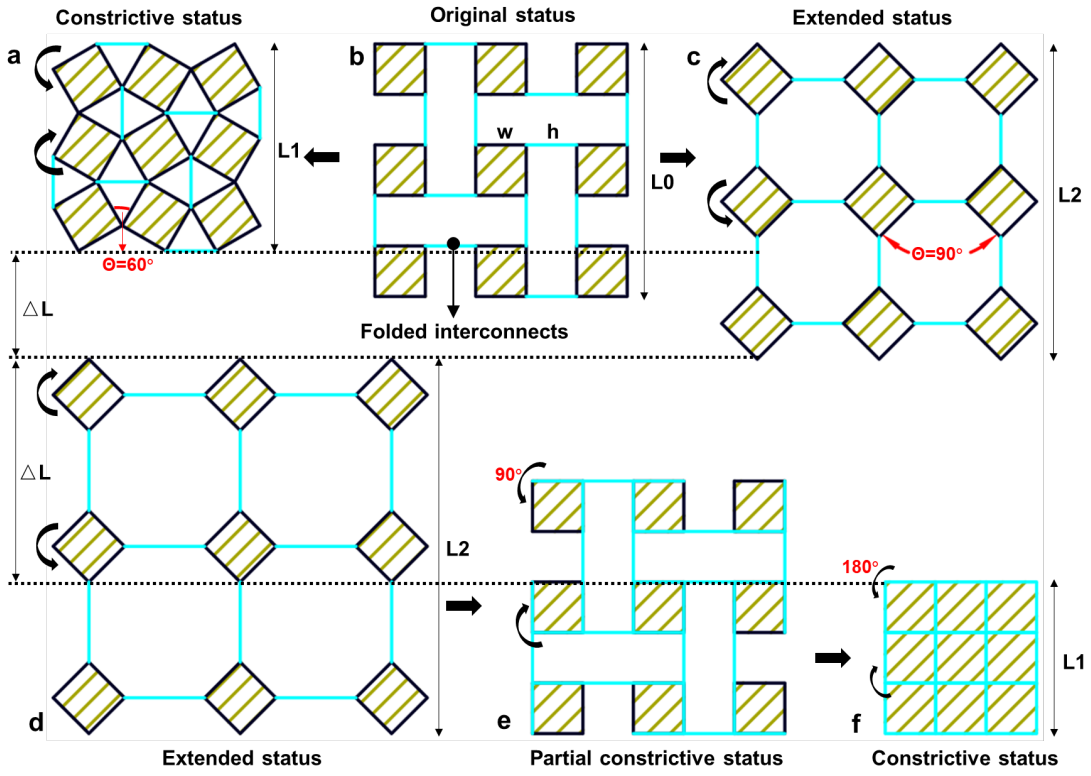

Supplementary Figure 5. **a b c** The constrictive, original, extended status of rotating squares structure with w = h. **d e f** The extended, partial constrictive, constrictive status of rotating squares structure with w = h/2.

Firstly, we set **w** = **h** (as shown in Supplementary Figure 5b). After folding the interconnects vertically (bright blue line), the area occupied by the interconnects becomes pores. Rotate the discrete squares to bring them together until self-intersecting occurs, where the corners of adjacent squares touch each other (when the angle between the adjacent squares is 60°, Supplementary Figure 5a), and the structure is compressed to the maximum. Instead, by rotating the squares away from each other (when the angle between the adjacent squares is 90°, Supplementary Figure 5c), the structure is stretched maximumly. We treat these two states as two self-locking states of the rotating square auxetic structure. In this case, with **n**, **w** and **h** as elements, the stretchability **S** can be geometrically defined as:

$$S = \frac{L_2 - L_1}{L_1} = \frac{\sqrt{2}nw + 2(n-1)w - (\sqrt{3}+1)nw/2}{(\sqrt{3}+1)nw/2} \quad (2)$$

If **h** is greater than **w**, let's set **h** = 2**w**, then the stretchability of the structure increases dramatically. As shown in the Supplementary Figure 5, the stretching process is the same as before, while the compression can be divided into two steps. In the first step, as the squares rotate 90° and move closer to each other, some of the previously exposed edges are covered with interconnects (from black lines to bright blue lines and into a partial constrictive status, Supplementary Figure 5e). As the squares rotate 180°, then all edges are covered by interconnects and called constrictive status (Supplementary Figure 5f). In this case, the stretchability **S** can be geometrically defined as:

$$S = \frac{\sqrt{2}nw + 2(n-1)w - nw}{nw} \tag{3}$$

Theoretically, with the increase of gap **h**, the stretchability of the structure can be infinitely improved, but this is meaningless for practical application. In addition, we analyzed the relationship between the stretchability and **n**, as shown in the figure below. Similar to the area utilization ratio, with the increase of **n**, the stretchability also tends to the respective theoretical values (Supplementary Figure 6).

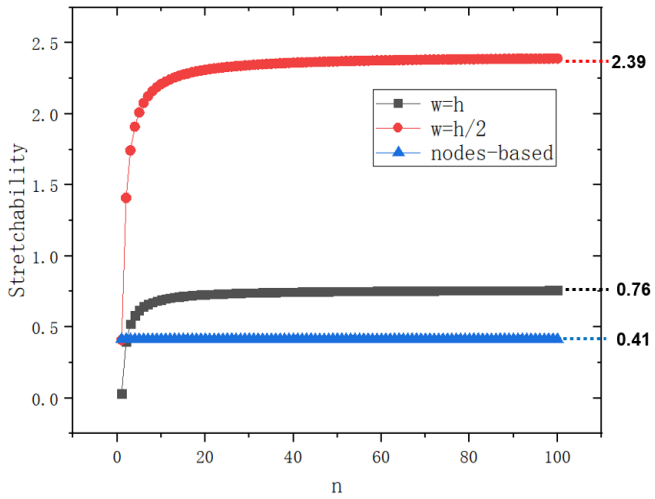

Supplementary Figure 6. Diagrams of relationships between n, w and h and comparison of stretchability with rigid nodes-connected structure.

Local tensile test was performed to verify the theoretical stretchability of the structure mentioned above. As shown in Supplementary Figure 7, the squares rotate and get close to each other by uniaxially squeezing part of the display. Different from the theoretical analysis, due to the self-intersecting of the flexible vertical interconnects (the interconnects touch each other as shown in the inset), the adjacent angle of the squares can only reach about 40° (less than the theoretical value of 45°). Similarly, when the display is partially uniaxial stretched, the interconnects cannot reach a straight configuration due to the bending stiffness (the interconnects present certain radian as shown in the inset). In the case of 4 × 6 pixels, the length and width are about 10mm and 15mm in constrictive status, respectively, and 15.3mm and 23mm in extended status. In this case, the biaxial strain $\varepsilon^x = \frac{X_{\max} - X_{\min}}{X_{\min}} = 54\%$, slightly lower than the

theoretical value of 58%. It is worth noting that, unlike auxetic structures connected by rigid nodes, local stretching or compression of the device does not result in global expansion or contraction. This is because the flexible interconnects can deform independently to absorb external energy, which entitles the device better impact resistance and improves durability.

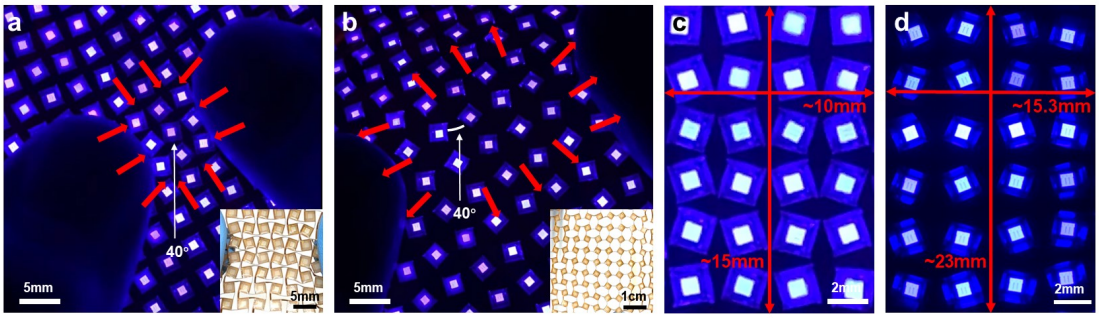

Supplementary Figure 7. **a b** The display is locally extruded and stretched, and the insets show optical pictures of the two states respectively. **c d** The constrictive, extended status of the device and the dimensions are marked with red line.

Viewing angle and luminance analysis

As mentioned in the article, while vertical interconnects bring benefits, they also limit the viewing angle of the display. Supplementary Figure 8a shows a schematic diagram of a single luminescent unit, the cross-sectional structure of its functional area (marked by green box) is illustrated in Supplementary Figure 8b. The viewing range is determined by the geometry of the luminescent unit. It is concise to calculate, according to the known geometric parameters, that when the angle (α) between the sight and the horizontal plane is 30°, pixels are obscured by vertical interconnects. The inset of Supplementary Figure 8b shows the folded crease stack-ups (marked by the red dotted ellipse) identified via different colors. We calculated the strain of outer circuit at crease by bending normal stress general formula to prove the reliability of vertical link structure. The outer copper reaches the maximum strain of 14% when the interconnect in the vertical configuration, which is less than the theoretical limit of 16% (IPC-2223E standard). Supplementary Figure 8c, d and e present optical images of lit display when α equal to 90°, 60° and 30°, respectively. The pixels in endmost area are blurry and disappearing (marked with red box) when α = 30° in Supplementary Figure 8e. 20mW DC power was used to drive a single luminescent unit and illuminometer was used to test its luminance from different tilt angles. The results show that the single luminescent unit can maintain its luminance at 17-22 cd/m^2 when α is greater than 30°, while less than 6 cd/m^2 when α is less than 30°.

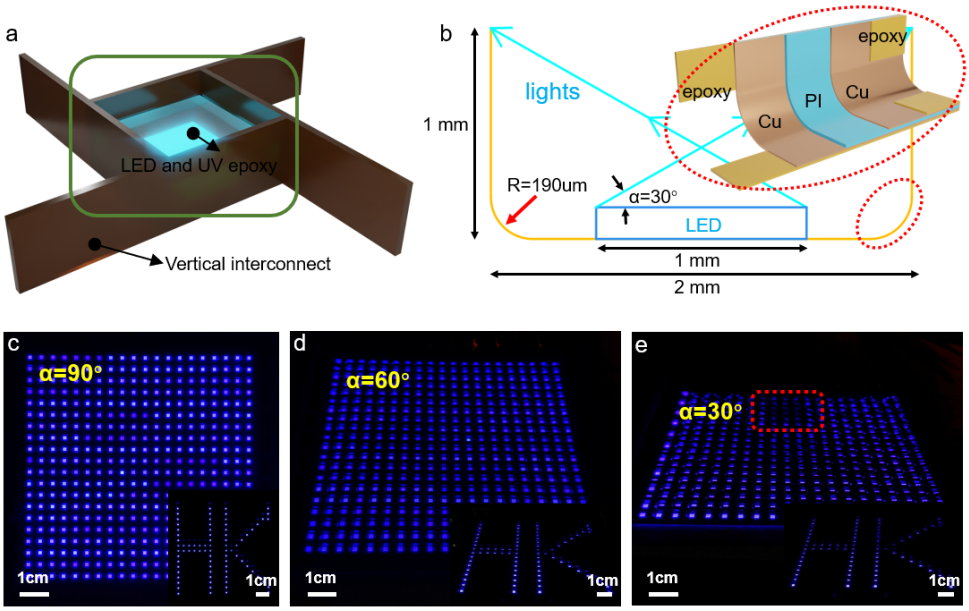

Supplementary Figure 8. Analysis of viewing range and crease reliability of luminescent units. **a** Rendering of single luminescent unit consists of four vertical interconnects, LED chip and UV epoxy. **b** The cross section diagram of the luminescent unit and layered rendering of the crease (inset). **c d e** Optical images of lit display in different viewing angle. Insets: letter pattern “HK” in accordance with each image.